Bivariate thermodynamics of multifractals as an eigenvalue problem

Zoltán Kovács
Institute for Theoretical Physics, Roland Eötvös University, Puskin u. 5-7, H-1088 Budapest, Hungary

Tamás Tél*
Institute for Theoretical Physics, Rheinisch-Westfalische Technische Hochschule Aachen, D-5100 Aachen and Institut für Festkörperforschung, Research Center Jülich, D-5170 Jülich, Federal Republic of Germany
(Received 26 June 1991)

A bivariate iteration scheme is introduced based on single-humped functions $f(x)$ and $g(y)$, which generate the length scales and their measures, respectively, according to a multifractal distribution. The largest eigenvalue of this procedure is connected with the Gibbs potential $G(\beta, q)$, from which dimensions, entropies, and Lyapunov exponents can be extracted. The mechanisms leading to phase transitions in the Gibbs potential and in multifractal spectra are analyzed. The method provides us with a general scheme for classifying possible phase transitions in multifractals. As a novel phenomenon in the field of dynamical systems, we study phase transitions in spectra belonging to the natural measure of nonhyperbolic repellers of one-dimensional maps.

PACS number(s): 05.45.+b, 05.70.Fh, 05.70.Ln, 64.60.Ak

I. INTRODUCTION

In analyzing strange sets, the application of thermodynamic formalism [1–9] has become a standard tool. This method provides us with an illuminating analogy between the hierarchical organization of fractals and the statistical mechanics of spin chains, and with a deeper understanding of singularities in multifractal spectra, which can be interpreted as phase transitions.

The free-energy function $F(\beta)$ is a central quantity of the formalism characterizing the scaling behavior of length scales [1, 5]. For fractals that can be covered by a refining set of d-dimensional balls, $F(\beta)$ is defined as follows: Let $l_i^{(n)}, i = 1, 2, \ldots$ denote the radii of the covering balls at level n. Take the partition function containing the sum over these length scales raised to some power β and obtain the free energy for large n via relation

$$Z_n(\beta) \equiv \sum_i l_i^{(n)\beta} \sim \exp[-\beta F(\beta) n]. \tag{1}$$

As a basic result, the fractal dimension D_0 of the set is just that particular value of β at which F vanishes: $F(\beta = D_0) = 0$. [In the mathematical literature $-\beta F(\beta)$ is called the topological pressure [1].]

A broad class of fractals embedded in one dimension (d=1) can be generated via a single-humped function $f(x)$ of the type shown in Fig. 1(a). The nth preimages of the function's support $I = [0, 1]$ of such *open* maps consist of intervals of length $l_i^{(n)}$ and approach a Cantor-like set for $n \to \infty$. The limiting set is sometimes called a "cookie cutter" [5]. The free energy of such fractals can best be studied by means of an eigenvalue problem [10, 11], which provides us with a mathematically convenient frame and numerically very fast convergence. The iterative version of this equation (generalized Frobenius-Perron equation [10–20]) has the form

$$\lambda(\beta) Q_{n+1}(x) = \sum_{\epsilon(=0,1)} \frac{Q_n(f_\epsilon^{-1}(x))}{|\, f'(f_\epsilon^{-1}(x))\,|^\beta}, \tag{2}$$

where ϵ is used to distinguish between the two branches of the inverse f^{-1}. Starting with any smooth and positive initial function $Q_0(x)$, one finds for each β a *unique* number $\lambda(\beta)$ (the largest eigenvalue) at which the iteration converges towards a *finite* limiting $Q(x)$ (the corresponding eigenfunction) for $n \to \infty$. It has been shown that $\lambda(\beta) = \exp[-\beta F(\beta)]$, i.e., the free energy can easily be obtained from eigenvalue $\lambda(\beta)$.

Often, there is something distributed on a fractal support. This stationary distribution defines a multifractal measure [21, 22] characterized by, among others, the spectrum of generalized dimensions D_q [23]. Besides exceptional cases (when, e.g., the measure of each ball is proportional to its radius), the free energy evaluated via the length scales of the support does *not* contain any information concerning the distribution. Consequently, dimensions D_q for $q \neq 0$ cannot be derived from $F(\beta)$. In order to describe general multifractal measures bivariate thermodynamic functions have been introduced [4, 7], [24–29]. We use here the so-called Gibbs potential $G(\beta, q)$ obtained from a double partition function containing both the length scales and the measures [4, 7]: Let $P_i^{(n)}$ denote the (normalized) measure, at generation n, falling in the ball of radius $l_i^{(n)}$. Consider the sum over all balls that contains the qth and βth powers of the measures and radii, respectively,

$$Z_n(\beta, q) \equiv \sum_i P_i^{(n)q} l_i^{(n)\beta}. \tag{3}$$

The Gibbs potential can then be read off from the relation

$$Z_n(\beta, q) \sim \exp[-\beta G(\beta, q) n], \tag{4}$$

valid for large n. The value of β at which G with a fixed q vanishes is just $(1-q)$ times the order-q dimension: $G(\beta=(1-q)D_q,q)=0$. Taking the Gibbs potential at $q=0$, the free energy is recovered.

We show that the Gibbs-potential description and the eigenvalue formalism can be combined. This is achieved if one defines, by means of two different maps, length scales and measures in one-to-one correspondence: Consider fractal supports generated by a function $f(x)$ as described above. Take another function $g(y)$ on $[0,1]$, define hierarchically a set of intervals in the same way as for $f(x)$, and consider the sizes of these intervals at a given level n as the *measures* of the length scales generated by $f(x)$ at the same level. We call f and g the *length scale map* and *measure map*, respectively. Due to the one-to-one correspondence between length scales and measures, the symbolic encoding [7] of these two sets has to be identical. This is obviously the case if both maps are open [like the one in Fig. 1(a)]. The normalization of the measure, however, would require then the introduction of an extra prefactor. In order to avoid this, we take—if not stated otherwise—the measure map to be a *closed* one mapping its support exactly onto itself [Fig. 1(b)]. The preimages of the support with respect to g cover then the entire interval $(0,1)$, i.e., normalization is automatically maintained. The iteration scheme belonging to this problem will be of the form:

$$\lambda(\beta,q)Q_{n+1}(x,y)=\sum_{\epsilon(=0,1)}\frac{Q_n(f_\epsilon^{-1}(x),g_\epsilon^{-1}(y))}{|f'(f_\epsilon^{-1}(x))|^\beta|g'(g_\epsilon^{-1}(y))|^q} \tag{5}$$

that we call the bivariate Frobenius-Perron equation. The definition of the largest eigenvalue $\lambda(\beta,q)$ is similar to that in (2): Starting with any smooth positive $Q_0(x,y)$, there is a unique $\lambda(\beta,q)$, so that the iteration converges towards a finite limiting $Q(x,y)$ for $n\to\infty$. We claim that in this case

$$\lambda(\beta,q)=\exp[-\beta G(\beta,q)], \tag{6}$$

which provides a powerful method for computing the Gibbs potential.

Let us briefly discuss under which conditions a measure map can (or cannot) be constructed explicitly. The preimages of the unit interval taken with respect to a closed symmetric tent map are all of equal length. Such a measure map associates, therefore, the same weight with all length scales (balanced measure). A g defined by two linear branches with different slopes generates a two-scale multiplicative measure, which is quite common in physical examples [8]. A piecewise-linear measure map possessing breakpoints in the first and second preimages of unity (having thus four different slopes) corresponds to a four-scale multiplicative measure. By considering maps with breakpoints in $2^n-1 (n>2)$ preimages of unity but being linear between them, one can generate multiplicative measures with arbitrarily many scales. The fact that $g(y)$ in Eq. (5) might be other than piecewise linear indicates that our framework allows for studying measures more general than multiplicative ones.

The choice of a measure map in the form of Fig. 1(b) also implies restrictions to the measures studied. Consider a general (binary coded) fractal measure defined by the weights $\{P_i^{(n)}, i=1,2,...,2^n\}$ at level n. One can always find a piecewise-linear $g(y)$ with 2^n-1 breakpoints so that the lengths of the nth preimages of $[0,1]$ are exactly these values. Apart from multiplicative cases, however, the next, $(n+1)$st level corresponds to another piecewise-linear map with $2^{n+1}-1$ breakpoints. The series of such maps need not, in general, possess a limit for $n\to\infty$, or if it does, the limiting map need not be sufficiently well behaved. Thus, the *existence* of a *smooth* measure map is not fulfilled in arbitrary cases. Never-

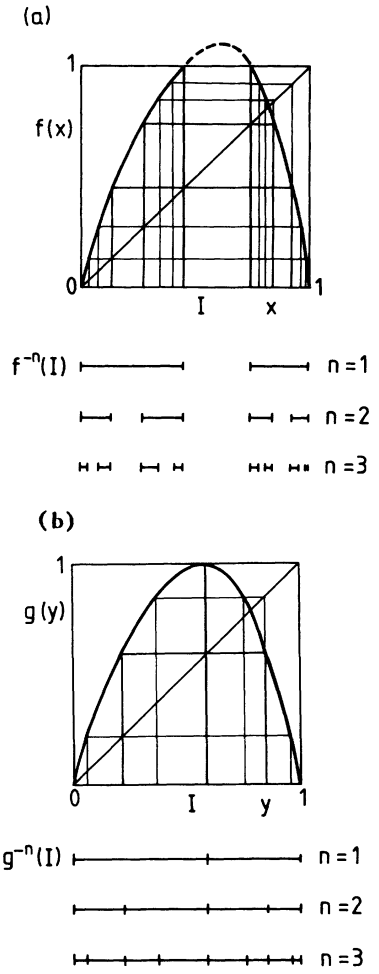

FIG. 1. Functions used as generators for length scales and measures. (a) An open map, having a maximum larger than unity, and the approximation of a "cookie cutter" via the preimages of its support $I=[0,1]$. (b) A closed map, having a maximum exactly at 1, and the partition of the unit interval via the preimages of the support. In both cases each nth preimage can be coded by a binary symbol sequence $\{\epsilon_i\}$ of length n containing 0's and 1's, and all possible codes are allowed to occur. Any given symbol sequence $\epsilon_1,\epsilon_2,...,\epsilon_n$ can be associated with a length scale and a measure as the size of the corresponding preimage of the unit interval taken with respect to f and g, respectively.

theless, the class characterized by this property is broad enough so that, by changing the form of $g(y)$, entire families of measures can be studied and one can hope to thus obtain new insight into the general properties of multifractals. (The existence of a length-scale map implies a similar restriction for the fractal supports.)

In the particularly important case of the natural invariant distribution of fully developed chaotic maps. the measure map $g(y)$ can always be constructed explicitly as shown in Sec. V A. It is worth mentioning, however, that certain general properties of multifractals (e.g., a nonexponential local scaling) can be modeled by suitably chosen measure maps that lead to a Gibbs potential with the same global features (e.g., singularities) as that of the original systems [e.g., diffusion-limited-aggregation (DLA) growth] where no measure map exists.

Our aim is, therefore, not so much the discussion of the proper choice of g for a given system but rather the setting up of a general framework to classify multifractal measures and their properties. In particular, we shall be interested in phase transitions [30–38] in the Gibbs potential and in the manner in which they are reflected in other spectra like generalized dimensions. By means of the bivariate Frobenbius-Perron equation we can show that there is a region, called the condensed phase, where $\beta G(\beta,q)$ is a linear function and depends on a few parameters of the maps f and g only. In this phase, spectra like generalized dimensions can be given explicitly. These properties of the Gibbs potential derived for cases characterized by measure maps are conjectured to hold for all systems exhibiting phase transitions in their D_q spectra.

From the point of view of dynamical systems, the natural invariant measure defined by a map $f(x)$ is of special importance, and it is possible to find a $g(y)$ corresponding to this measure. The investigations of natural measures by means of Eq. (5) shed new light on the mechanism of phase transitions in the dimensions of chaotic attractors. We demonstrate that similar transitions also occur in the case of *nonhyperbolic* chaotic *repellers*, and determine their properties.

The paper is organized as follows. Section II gives a brief summary of the properties of the Gibbs potential $G(\beta,q)$. The derivation of the eigenvalue equation is discussed in Sec. III (technical details are relegated to the Appendix). Next, we analyze how singularities of the eigenfunction are built up under iteration, specify an anomalous eigenvalue, and find the condition for first-order and exotic phase transitions in G and in related spectra (Sec. IV). The application to the natural measure of one-dimensional chaotic attractors and repellers is given in Sec. V. Since this last part assumes some knowledge concerning dynamical systems, readers interested only in the general aspects of multifractals may jump directly to the concluding Sec. VI.

II. THE GIBBS POTENTIAL

First, let us briefly summarize the thermodynamic interpretation of $G(\beta,q)$. Both the length and the measure of a given box at level n are associated with the same symbol sequence $\{\epsilon_1,\epsilon_2,...,\epsilon_n\}$. Since the functions f and g are single humped, the symbols are binary, and ϵ_i can take on two values (0 or 1). Note that each symbol sequence and therefore each box corresponds to a *microstate of an Ising chain* of length n. By increasing the resolution, both the length scales and the measures tend to zero. For large n one can thus write [1]

$$l_i^{(n)} \sim \exp(-E_i n) \quad \text{and} \quad P_i^{(n)} \sim \exp(-L_i n), \tag{7}$$

where the quantities E and L depend on the particular symbol sequence but stay finite in the limit $n \to \infty$. After substitution, Eq. (3) can be interpreted as the partition function of an elastic Ising chain with long-range and multispin interactions in the T-p ensemble: E and L correspond to the energy and length (per spin) of a microstate, respectively, and β and q play the role of intensive parameters (the inverse temperature and pressure). The limit $n \to \infty$ is the thermodynamic limit, and correspondingly, $G(\beta,q)$ is the Gibbs potential (density) of the Ising chain. The bivariate Legendre transform of the Gibbs potential can be interpreted as an entropy function [4, 38, 29] directly related to $f(\alpha)$-type multifractal spectra [21]. In what follows we shall not use this analogy in detail, but note that any nonanalytic behavior in G of a multifractal measure corresponds to a phase transition in an associated elastic Ising chain.

General multifractal measures are conventionally characterized by three independent spectra: those of generalized dimensions [23], entropies [39], and Lyapunov exponents [40]. We show next how they can be derived from the Gibbs potential.

Order-q dimensions have been shown to follow from the relation [21]

$$\sum_i \frac{P_i^{(n)q}}{l_i^{(n)(q-1)D_q}} \sim 1 \tag{8}$$

as $n \to \infty$. A comparison with Eq. (4) then leads to

$$G(\beta,q)|_{\beta=(1-q)D_q} = 0. \tag{9}$$

The next two spectra have originally been introduced in connection with chaotic motion generated under the iteration of some maps but they can be used for any multifractal. Generalized entropies K_q reflect purely probabilistic properties and are defined [39, 3] via

$$\sum_i P_i^{(n)q} \sim \exp[(1-q)K_q n] \tag{10}$$

for large n. Consequently,

$$\beta G(\beta,q)|_{\beta=0} = (q-1)K_q, \tag{11}$$

i.e., the entropy spectrum is contained by the $\beta = 0$ line of the Gibbs potential.

Generalized Lyapunov exponents λ_q characterize the distribution of expansion factors $\Lambda_i^{(n)}$ which tell us how rapidly small pieces are blown up to size of order unity under map $f(x)$. Take their power q and average with respect to the measure. This defines [40, 41] λ_q according to

$$\sum_i \Lambda_i^{(n)q} P_i^{(n)} \sim \exp(q\lambda_q n). \tag{12}$$

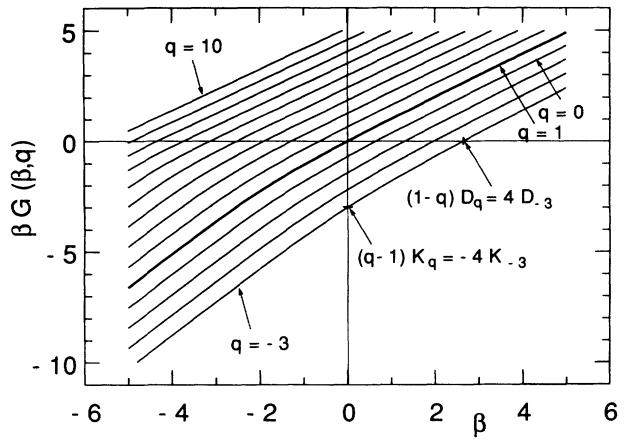

FIG. 2. The graph $\beta G(\beta, q)$ vs β taken at different fixed values of $q = -3, -2, ..., 10$. It is shown how dimensions, entropies, and Lyapunov exponents can be read off from this plot. The diagram has been obtained by solving Eqs. (5) and (6) as described in Sec. III C by taking $f(x) = 4.5x(1-x)$, and $g(y) = 5y/2$ for $y < 0.4$ and $g(y) = 5(1-y)/3$, otherwise. The heavy line passing through the origin is the graph of the Lyapunov spectrum $\beta G(\beta, 1) = \beta\lambda_{-\beta}$. The one below is the free energy $\beta F(\beta)$.

The average Lyapunov exponent is $\bar{\lambda} \equiv \lambda_{q\to 0}$. In our case the expansion factors are just the reciprocal values of the length scales: $\Lambda_i^{(n)} = 1/l_i^{(n)}$; nevertheless, the spectrum of λ_q differs from $F(\beta)$ since an average is taken now with respect to $P_i^{(n)}$. We thus find

$$G(-q, 1) = \lambda_q. \tag{13}$$

The relations above imply that the order-q dimension D_q and entropy K_q can be read off from the intersections of the plot $\beta G(\beta, q)$ vs β with the horizontal and vertical axes, respectively (Fig. 2). The curve with $q = 1$ corresponds to the Lyapunov spectrum. All this shows that the entire Gibbs potential contains much more information than conventional spectra. It provides, in fact, the most general characterization of multifractals in the thermodynamic sense.

Finally, we note that by taking the limit $q \to 1$ one obtains a connection between the metric entropy and information dimension

$$K_1 = \lambda_0 D_1 \tag{14}$$

valid for any measure [41].

III. THE BIVARIATE FROBENIUS-PERRON EQUATION

A. Hyperbolic cases

The derivation of Eq. (6) is rather easy for hyperbolic cases. Hyperbolicity means that the n-fold iterated maps f^n and g^n are expanding and have finite slopes in *all* points of the invariant sets under f and g, for n sufficiently large. This implies that the measure map must have a locally linear maximum on its support $I = [0, 1]$.

As mentioned in the Introduction, we consider length scales and measures defined hierarchically by the preimages of the support I taken with respect to the maps f and g, respectively. At level n one thus has

$$l_i^{(n)} = f_i^{-n}(I) \quad \text{and} \quad P_i^{(n)} = g_i^{-n}(I), \tag{15}$$

$i = 1, ..., 2^n$ as illustrated in Fig. 1, where g is a closed map. A multifractal distribution obtained in this manner is plotted in Fig. 3. It is worth stressing that the measure generated by an arbitrarily chosen $g(y)$ *differs* from the natural measure of the length-scale map considered as a dynamical system $x_{n+1} = f(x_n)$. In fact, the length-scale and measure maps are used here as generating functions for the support and the weights of a multifractal; the dynamics defined by $f(x)$ or $g(y)$ do *not* play any role in the discussion. [In cases when the length-scale map is known and the measure is the natural measure induced by this map, $g(y)$ is no longer independent of $f(x)$, as will be discussed in Sec. V.] The measure map used in Fig. 3 generates a two-scale multiplicative measure on a fractal support. This might be contrasted with the natural measure corresponding to the hyperbolic repeller of the map $x_{n+1} = f(x_n)$ which would be proportional to the length scales: $P_i^{(n)} \sim l_i^{(n)}$ at each level. A nonmultiplicative measure defined by another $g(y)$ on the same support is given in Fig. 4.

The length scales $l_i^{(n)}$ are just the intervals on which the function f^n is monotonic. Due to hyperbolicity, there are no folds or cusps on these intervals, and the graph of f^n can be approximated on each such piece by a straight line with a slope of $f^{n\prime}(\bar{x}_i)$ where $\bar{x}_i$ can be any point inside the interval. Since the interval is mapped onto I in n steps, we can express the length scales $l_i^{(n)}$ approximately as

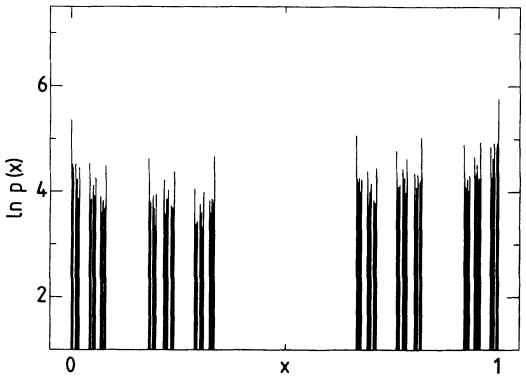

FIG. 3. Multifractal distribution obtained by applying rule (15) at level $n = 10$. The length scale and the measure maps are the same as in Fig. 2. The sizes of the tenth preimages of $I = [0, 1]$ with respect to $g(y)$ were taken as measures $P_i^{(n)}$ of the length scales $l_i^{(n)}$'s. The latter are generated as the tenth preimages of I with respect to $f(x)$. The logarithm of the density $p(x) = P_i^{(n)}/l_i^{(n)}$ for $x \in f_i^{-n}(I)$ is plotted. The Gibbs potential belonging to this measure is shown in Fig. 2.

$$l_i^{(n)} \sim \frac{1}{|\, f^{n\prime}(\bar{x}_i)\,|}. \tag{16}$$

Analogously, if g is also hyperbolic, one obtains

$$P_i^{(n)} \sim \frac{1}{|\, g^{n\prime}(\bar{y}_i)\,|}, \tag{17}$$

with $\bar{y}_i$ as an arbitrary point inside the interval $g_i^{-n}(I)$.

Next, iterate Eq. (5) n times to connect $Q_n(x,y)$ with the initial function. The resulting equation contains the n-fold iterates f^n, g^n on the right-hand side:

$$\lambda^n(\beta,q)Q_n(x,y) = \sum_{i=1}^{2^n} \frac{Q_0(x_i,y_i)}{|\, f^{n\prime}(x_i)\,|^{\beta}|\, g^{n\prime}(y_i)\,|^{q}}, \tag{18}$$

where x_i and y_i are the nth preimages of x and y, respectively, *taken along the same symbolic path.* This can be best expressed by the following notation. Let F_ϵ and G_ϵ denote the inverse of the length scale and measure map, respectively:

$$F_\epsilon = f_\epsilon^{-1} \quad \text{and} \quad G_\epsilon = g_\epsilon^{-1}, \tag{19}$$

with the convention that $\epsilon = 0$ denote the increasing branch of f or g. F_ϵ's have been termed the presentation functions of the fractal support [16]. Analogously, we call G_ϵ's the *presentation functions for the measure.* The preimages appearing in (18) can then be written as

$$\begin{aligned} x_i &= F_{\epsilon_1} \circ F_{\epsilon_2} \circ \cdots \circ F_{\epsilon_n}(x), \\ y_i &= G_{\epsilon_1} \circ G_{\epsilon_2} \circ \cdots \circ G_{\epsilon_n}(y), \end{aligned} \tag{20}$$

where all ϵ_i's can take on the values 0 or 1.

Since $\lambda(\beta,q)$ is defined by requiring the existence of a finite limiting function $Q(x,y)$, we can rewrite (18) for large n as

$$\lambda^n(\beta,q) = \frac{1}{Q(x,y)} \sum_{i=1}^{2^n} \frac{Q_0(x_i,y_i)}{|\, f^{n\prime}(x_i)\,|^{\beta}|\, g^{n\prime}(y_i)\,|^{q}}. \tag{21}$$

Taking the initial function to be the identity, which can be done due to the uniqueness of the solution when starting with smooth functions, one finds that $\lambda(\beta,q)$ is expressible by a partition sum

$$Z_n(\beta,q;x,y) = \sum_{i=1}^{2^n} \frac{1}{|\, f^{n\prime}(x_i)\,|^{\beta}|\, g^{n\prime}(y_i)\,|^{q}} \tag{22}$$

as

$$Z_n(\beta,q;x,y) \sim \lambda(\beta,q)^n. \tag{23}$$

Putting the length scales (16) and measures (17) into relation (3) and comparing with (22) we find for large n

$$Z_n(\beta,q) \sim Z_n(\beta,q;x,y), \tag{24}$$

which implies Eq. (6).

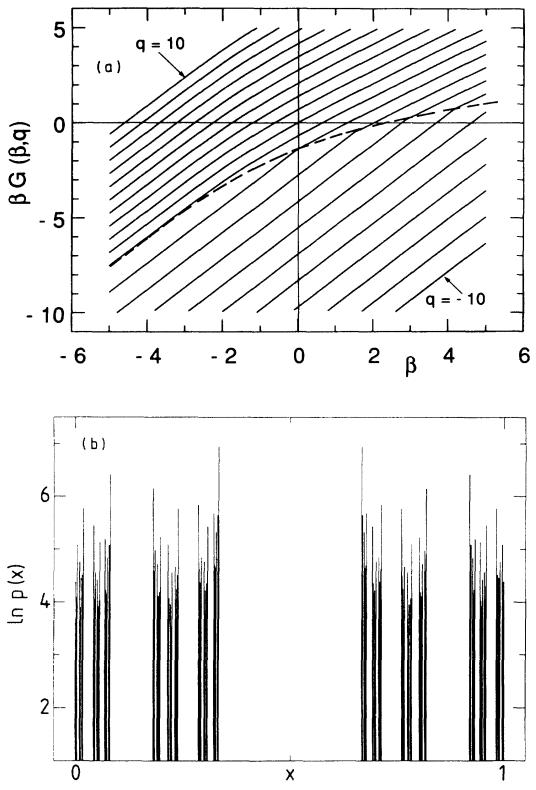

FIG. 4. (a) Generic phase transition in the Gibbs potential for $q = -10, \ldots, 10$. In this particular case $f(x) = 4.5x(1-x)$, $g(y) = 4y(1-y)$ is taken. The plot was obtained by numerically computing $G_1(\beta,q)$ from generations $n = 7, 8$ as described in Secs. IV A and III C, and by using relations (31) and (32). The maximum error is of the order of 0.01. The dashed curve denotes the critical line. Note that the fractal support in this problem and in the example of Fig. 2 is identical; differences in the plots are due to the measures. (b) Multifractal distribution corresponding to the length scale and measure maps given above obtained by applying rule (15) at $n = 10$. Note that no essential difference between this plot and that of Fig. 3 can be observed. The phase transition reflects the anomalous (but exponential) scaling of length or measure of a few boxes and can, therefore, be seen only if subsequent levels n are compared.

B. Nonhyperbolic cases

The arguments of Sec. III A do not apply if the length scale and measure maps have local extrema or singularities on their invariant sets. Such nonhyperbolic cases have to be investigated more carefully. The derivation of Eqs. (5) and (6) is then technically more involved; therefore, we relegate it to the Appendix.

C. Numerical determination of the eigenvalue $\lambda(\beta,q)$

The easiest way to extract the largest eigenvalue $\lambda(\beta,q)$ of the bivariate Frobenius-Perron equation numerically is based, in both hyperbolic and nonhyperbolic cases, on the partition sum (22). We can write (23) as

$$\ln \lambda(\beta,q) \approx \ln Z_n(\beta,q;x,y) - \ln Z_{n-1}(\beta,q;x,y). \tag{25}$$

The dependence on x, y disappears for large n, provided

they lie inside the support I. The computation of the partition sum (22) built on a complete binary tree is numerically very easy. In the knowlegde of the eigenvalue, the eigenfunction can then be constructed via Eq. (21) as $Q(x,y) = \lambda^{-n}(\beta,q)Z_n(\beta,q;x,y)$. As an estimate to the error of this algorithm at level n we use the quantity $\ln(Z_nZ_{n-2}/{Z_{n-1}}^2)$. The convergence is typically exponentially fast, and we find an accuracy of order 10^{-2} already at $n = 8$ in the entire range $|\beta|, |q| < 5$ for hyperbolic cases. The convergence is much worse around phase-transition points, but this can be avoided by using well-suited singular initial functions, as discussed in the next section, leading to accuracies similar to the above.

IV. PHASE TRANSITIONS

A. Singularity analysis: Generic transitions

If either the length scale or the measure map is nonhyperbolic, of the type shown in Fig. 1(b), a typical phase transition occurs in the Gibbs potential (Fig. 4). Essential features of this transition depend solely on the order of the maximum and on the slopes taken at the two end points of the support. Let the exponents z and z' denote the orders of maxima of f and g, respectively. A smooth maximum and a cusp correspond to an exponent greater and less than unity, respectively. For simplicity, we restrict our investigations to maps without cusps, i.e., $z, z' \geq 1$. The case of a maximum outside the support (hyperbolicity) corresponds to a class where the exponent is unity. In addition, the slopes of the function f (g) at $x = 0$ and 1 will be denoted by c (c') and c_1 (c_1'), respectively (see Fig. 5).

The appearance of the phase transition can be understood by following how singularities are built up in the iteration scheme (5). The analysis is an extension of the method applied in the single-variable problem [18]. The most important steps are as follows: Start with $Q_0(x,y) \equiv 1$. In the first iteration, a singularity shows up at $x, y = 1$:

$$Q_1(x \to 1, y \to 1) \sim (1-x)^{-\sigma(\beta)}(1-y)^{-\sigma'(q)} \quad (26)$$

with

$$\sigma(\beta) = (1 - 1/z)\beta, \qquad \sigma'(\beta) = (1 - 1/z')q. \quad (27)$$

Otherwise, Q_1 stays smooth on the unit square. In the next step, the singularity does not change around $x, y = 1$. As a consequence, the application of (5) around the origin yields that

$$\lambda(\beta,q)Q_2(x \ll 1, y \ll 1) = \frac{A}{c^\beta c'^q} + \frac{Bx^{-\sigma(\beta)}y^{-\sigma'(q)}}{{c_1}^\beta {c_1'}^q}, \quad (28)$$

where A, B are constants. If both σ and σ' are positive, the second term dominates and the same singularity is created around the origin as around $x, y = 1$, and this remains so in subsequent iterations. The situation is completely different, however, if either $\sigma(\beta)$ or $\sigma'(q)$ is negative. Taking the limit $x \to 0$ ($y \to 0$) if $\sigma < 0$ ($\sigma' < 0$), one finds the first term to be dominant and, consequently, Q_2 has a finite value at $x = 0$ ($y = 0$). Since this property might be unaltered upon further iterations, we conclude that

$$\lambda_0(\beta,q) \equiv \exp[-\beta G_0(\beta,q)] = c^{-\beta}c'^{-q} \quad (29)$$

is a possible eigenvalue. For maps with $z, z' \geq 1$ this eigenvalue can exist only for $\beta < 0$ (if f is nonhyperbolic) or for $q < 0$ (if g is nonhyperbolic).

This argument also shows that when starting with an initial function having singularities of type σ at $x = 0, 1$ and of type σ' at $y = 0, 1$, like, e.g.,

$$Q_0(x,y) = [x(1-x)]^{-\sigma(\beta)}[y(1-y)]^{-\sigma'(q)}, \quad (30)$$

the nth iteration will also have the same singularities, and the eigenvalue $\lambda_0(\beta,q)$ does not show up then [18]. The eigenvalue $\lambda_1(\beta,q) \equiv \exp[-\beta G_1(\beta,q)]$ ensuring convergence in this class can easily be obtained by using the numerical procedure described in Sec. III C applied to Eq. (18), with Q_0 as given by (30).

Let us turn back now to smooth initial functions. We have seen that there is a range of β and q where the function $Q_n(x,y)$ has the same singularities as (30) and, therefore, $\lambda(\beta,q) = \lambda_1(\beta,q)$ there. However, in the range where $\lambda_0(\beta,q)$ exceeds $\lambda_1(\beta,q)$, the former drives iterations towards a smooth function. Thus, the actual largest eigenvalue is the *maximum* of $\lambda_0(\beta,q)$ and $\lambda_1(\beta,q)$. The Gibbs potential is obtained, therefore, as

$$\beta G(\beta,q) = \min[\beta G_0(\beta,q), \beta G_1(\beta,q)], \quad (31)$$

where both G_0 and G_1 are smooth functions.

At points where the branches intersect each other, a break shows up in the plot of the Gibbs potential. This occurs at a q-dependent critical inverse temperature $\beta_c(q)$ defined by $G_0(\beta_c(q),q) = G_1(\beta_c(q),q)$, and corresponds to a first-order transition since the first derivative of G is discontinuous. In the range where $\lambda(\beta,q) = \lambda_0(\beta,q)$, the Gibbs potential is explicitly known:

$$\beta G(\beta,q) = \beta G_0(\beta,q) \equiv \beta \ln c + q \ln c'. \quad (32)$$

This is due to the fact that this contribution comes solely from points around the origin [see (28)]. Note that the nonhyperbolicity of either the length scale or the measure map is sufficient to induce this behavior. We call the region where (32) holds, the *condensed phase*. The complementer regime in which the presence of a nonlinear local maximum does not play an essential role can be called the *hyperbolic phase*. Furthermore, function G_1,

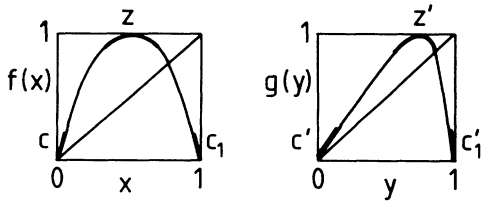

FIG. 5. Nonhyperbolic functions f and g and their parameters relevant in the singularity analysis: the orders of local maxima (z, z'), the slopes at the origin (c, c') and at unity (c_1, c_1').

differing from G in the condensed phase, can be considered to be a hyperbolic Gibbs potential not containing contributions from the origin.

The results for the total Gibbs potential shown in Fig. 4 are obtained in a case where the fractal support (f) is hyperbolic but the measure is not. Phase transitions appear here for negative values of q only.

B. Phase transitions in multifractal spectra

Let us define a *critical line* connecting the phase transition points on the $[\beta, \beta G(\beta, q)]$ plane (dashed line in Fig. 4). Whether there is a singularity in the spectra of dimensions, entropies, or Lyapunov exponents depends on the actual position of the critical line.

If the critical line intersects the β axis, there exists a critical value q_c so that the contributions of $G_0(\beta, q_c)$ and $G_1(\beta, q_c)$ become equal just when they are zero (Fig. 6). Consequently, the dimensions D_q belonging to q values smaller and larger than q_c can be read off from different branches. Therefore, the derivative of D_q is discontinuous at the critical point of q_c where $\beta_c(q_c) = (1-q_c)D_{q_c}$. Furthermore, since the branch G_0 is known, an explicit expression can be derived for the dimensions in the condensed phase. Using (9) and (32) we find that

$$D_q = \frac{q}{q-1}\frac{\ln c'}{\ln c}. \tag{33}$$

This result is universal since it contains the slopes of the length scale and measure maps only. It explains from a general point of view why the $q/(q-1)$ dependence is so common in dimension spectra with phase transition [30, 21]. In the example of Fig. 4 the condensed phase shows up at negative values of q, and relation (33) holds for $q \le q_c = -2.742$. Dimensions belonging to the hyperbolic phase have been determined numerically from the intersections of the Gibbs potential with the horizontal axis. The result is shown in Fig. 7.

In an analogous way we find that the entropy spectrum has a discontinuity in its derivative if the critical line intersects the vertical axis for some q_c' (Fig. 6). From (11) and (32), then, it follows that the entropies behave in the condensed phase as

$$K_q = \frac{q}{q-1}\ln c', \tag{34}$$

which depends solely on the slope of the measure map. In the example of Fig. 4 the critical value is $q_c' = -1$ and (34) holds for $q \le q_c$.

It is worth noting that the entropy spectrum is, by construction, always connected with the free energy $F_g(\beta)$ of the measure map. The bivariate Frobenius-Perron equation and relation (11) imply that

$$K_q = \frac{qF_g(q)}{q-1}. \tag{35}$$

A phase transition in the entropy spectrum can thus be present only if there is a phase transition in the free energy of g. In the case shown in Fig. 4 the measure map is the logistic parabola that has a transition in its free energy at $\beta_c = -1$. It is also known [31] that $\beta F_g(\beta) = (\beta - 1)\ln 2$ for $\beta > -1$, and thus in this special case we can determine the complete entropy spectrum in the hyperbolic phase, too, yielding $K_q = \ln 2$ for $q > -1$.

Finally, if the critical line intersects the $q = 1$ curve of the Gibbs potential (Fig. 6) at some $\beta_c(1)$, the Lyapunov spectrum has different right and left derivatives at $q_c'' \equiv -\beta_c(1)$. In the condensed phase an explicit result is obtained again:

$$\lambda_q = \ln c - \ln(c')/q, \tag{36}$$

as follows from (13) and (32). In the example of Fig. 4 no phase transitions can be present for positive values of q; therefore, the Lyapunov spectrum is smooth.

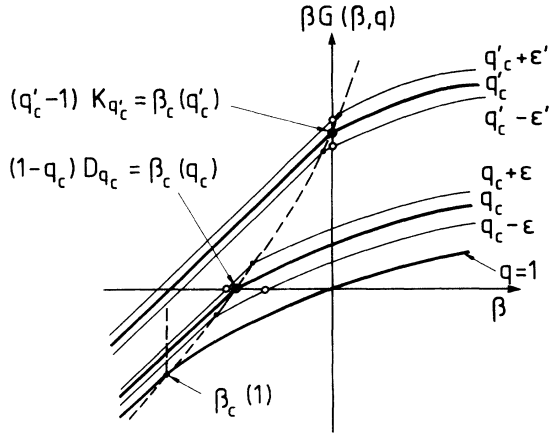

FIG. 6. Schematic illustration of the mechanism leading to phase transitions in the D_q, K_q, and λ_q spectra. The dashed curve stands for the critical line. The nondifferentiability of D_q (K_q) at q_c (q_c') follows from the fact that the Gibbs potential intersects the horizontal (vertical) axis with branches of different local character (G_0 or G_1) above and below the critical q value.

C. An upper bound to the Gibbs potential: Exotic transitions

We first derive a lower bound to the eigenvalue $\lambda_1(\beta, q)$ belonging to initial functions of type (30) by extending

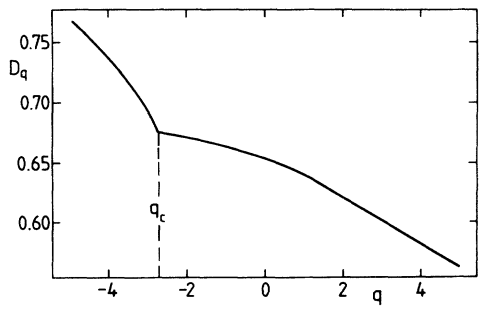

FIG. 7. The D_q spectrum as read off from Fig.4. In the condensed phase $q < q_c = -2.742$, $D_q = q/(q-1)\ln 4/\ln 4.5$ [see (33)].

the result obtained for the free energy [20]. In view of (31), this will also be an upper bound to the Gibbs potential. The n-fold iterated bivariate Frobenius-Perron equation (18), when applied to an initial function having the same singularities as (30), implies that for large n

$$\ln \lambda_1(\beta,q) \sim \frac{1}{n} \ln \sum_{i=1}^{2^n} \frac{Q_0(x_i,y_i)}{|\, f^{n\prime}(x_i)\,|^{\beta} |\, g^{n\prime}(y_i)\,|^{q}}. \tag{37}$$

We underestimate $\lambda_1(\beta,q)$ by keeping the $i=1$ term of the sum only where x_1 and y_1 are just the nth preimages (of some x and y) closest to the origin:

$$\ln \lambda_1(\beta,q) \geq \frac{1}{n} \ln \frac{Q_0(x_1,y_1)}{|\, f^{n\prime}(x_1)\,|^{\beta} |\, g^{n\prime}(y_1)\,|^{q}}. \tag{38}$$

The manner in which these special coordinates tend to zero for large n is determined by the slopes c, c': $x_1 \sim c^{-n}$, $y_1 \sim c'^{-n}$. Since around the origin, $Q_0(x,y,) \sim x^{-(1-1/z)\beta} y^{-(1-1/z')q}$, we find

$$\frac{Q_0(x_1,y_1)}{|\, f^{n\prime}(x_1)\,|^{\beta} |\, g^{n\prime}(y_1)\,|^{q}} \sim c^{-n\beta/z} c'^{-nq/z'}, \tag{39}$$

from which

$$\beta G(\beta,q) \leq \frac{\beta}{z} \ln c + \frac{q}{z'} \ln c' \tag{40}$$

follows. This upper bound is valid for both hyperbolic and nonhyperbolic cases at any β and q values. In fact, it often seems to be a rather close bound, yielding either the left or the right asymptotes of the graph of $\beta G(\beta,q)$ vs β.

The existence of the upper bound (40) might be of drastic consequence for the Gibbs potential if any of the slopes c or c' is unity or infinite. The function $\beta G(\beta,q)$ can then be forced to be a finite or infinite constant in entire range of its variables. Note that such exotic behavior shows up if either the length scale or the measure map is intermittent (unit slope) or extremely unstable (infinite slope).

From four different possibilities we choose here one exotic transition to discuss in some detail. Other exotic transitions can be analyzed in an analogous way. Let us assume that the measure map has an extremely unstable fixed point at the origin: $\ln c' = \infty$. Consequently, the weight of interval $i=1$ is very small; it decreases faster than exponentially with n. Equation (40) then implies that $\beta G(\beta,q) = -\infty$ for negative values of q. At $q=-0$ a phase transition occurs which sets in with an infinite jump in the Gibbs potential. The potential at $q=0$ is still finite since the support is well behaving.

As a consequence, both the dimension and entropy spectra are well defined for non-negative q only. Formally, $D_q = K_q = \infty$ for $q < 0$. This extraordinary behavior is reflected in the fact that the multifractal spectrum [21] $f(\alpha)$ is left-sided, i.e., consists of a single increasing branch which has its maximum at $\alpha = \infty$. The usual descending branch is completely missing. The existence of such a transition was first discussed on general grounds in Ref. [34]. Recent investigations of growth phenomena [43] provide evidence for its occurrence in the generalized dimensions of DLA clusters computed with respect to their growth probabilities. The absence of finite dimensions at negative q is a consequence of the fact that fjords are completely screened.

V. PHASE TRANSITIONS IN THE NATURAL MEASURES OF NONHYPERBOLIC CHAOTIC MAPS

A. Chaotic attractors

It has long been known that the dimension spectra of one-dimensional nonhyperbolic maps taken with respect to their natural measures exhibit a phase transition [30]. The phase transition found in the free energy of the same system [18] is completely different since this quantity contains geometrical information only. Our present approach enables us to connect these transitions and show that the nonanalytic behavior of the dimensions arises as a phase transition in $G(\beta,q)$ at a specific value q_c, which is of the same type as that in the free energy.

First, we have to specify the function g generating the natural measure. It was shown [42] that one can associate with each nonhyperbolic map f of the type shown in Fig. 1(b) a hyperbolic one $\tilde{f}$, also defined on $[0,1]$, the natural measure of which has a constant density. Since this connection is facilitated by conjugation, the length scales generated by $\tilde{f}^{-n}(I)$ are just the measures of the intervals obtained as the nth preimages of the support with respect to f. Thus, $\tilde{f}$ is exactly the measure map g.

The result of Ref. [42] says that $\tilde{f}$ is obtained as

$$\tilde{f}(x) = H(f(H^{-1}(x))) \tag{41}$$

where the conjugating function H is just the integral of the invariant density $\varrho(x)$ of map $f(x)$:

$$H(x) = \int_0^x \varrho(z)dz. \tag{42}$$

Let us, next, specify the Gibbs potential in the condensed phase. To this end, it is sufficient to determine the slope $\tilde{c}$ of the measure map $\tilde{f}$ around the origin. The invariant density is the stationary solution of the original Frobenius-Perron equation that corresponds to the $\beta=1$, $q=0$ case of Eq. (5). The singularity analysis of Sec. IV A shows that for a map $f(x)$ with order-z maximum $\varrho(x) \sim x^{-1+1/z}$ around the origin. Consequently, $H^{-1}(x) = (x/C)^z$ with C as a constant. Equation (41) then yields $\tilde{f}(x) = c^{1/z}x$ for $x \to 0$, where c is the slope of $f(x)$ at the origin. We can now apply relation (32) with $c' = \tilde{c} = c^{1/z}$ and find in the condensed phase

$$\beta G_0(\beta,q) = \left(\beta + \frac{q}{z}\right) \ln c \tag{43}$$

for the natural measure of nonhyperbolic maps.

Fortunately, the Gibbs potential in the hyperbolic phase can be determined without constructing the map $\tilde{f}$ explicitly, which might be cumbersome. We apply the following argument: As one knows, the contribution from the end points $x = 0,1$ is negligible in the hyperbolic

phase. Consequently, the largest eigenvalue $\lambda(\beta,q)$ is the same as the one obtained with initial functions of the type (30): $\lambda(\beta,q) = \lambda_1(\beta,q)$. Since the singularity of the measure shows up in the two end points of the support only, the measure must have a smooth density in all boxes outside a small neighborhood of 0 or 1. The measures of such boxes are thus proportional to their lengths. Consequently, apart from the end points, the map f itself is equally well suited for generating the measure as $\bar{f}$. Taking identical points $x = y$ in the bivariate Frobenius-Perron equation, we can write relation (18) as

$$\ln \lambda_1(\beta,q) \sim \frac{1}{n} \ln \sum{}' \frac{1}{|f^{n\prime}(x_i)|^{\beta+q}}, \tag{44}$$

where $\sum'$ stands for a restricted summation not containing contributions from a small but n-independent neighborhood of 0 or 1. The right-hand side is just $-\beta F_1(\beta)$, where $F_1(\beta)$ is the hyperbolic free energy characterizing the length-scale distribution by disregarding the extremal boxes. Since $\lambda_1(\beta,q)$ is connected with the Gibbs potential in the hyperbolic phase as $\lambda_1(\beta,q) = \exp[-\beta G_1(\beta,q)]$, we find

$$\beta G_1(\beta,q) = sF_1(s)\,|_{s=\beta+q}\,. \tag{45}$$

This means that the constant-q lines of the potential can simply be obtained by shifting the graph of $\beta F_1(\beta)$ along the β axis.

In the particular example of the logistic map $f(x) = 4x(1-x)$, the free energy F_1 is explicitly known and therefore $\beta G_1(\beta,q) = (\beta+q-1)\ln 2$. Using (43) one finds that the critical line is parallel to the vertical axis and lies at $\beta = -1$. In more general cases the critical line is less regular (Fig. 8).

The critical value q_c belonging to the break in the dimension spectrum is reached when $G_1(\beta_c(q_c),q_c) = 0$. Since the attractor is always an interval of fractal dimension 1, $F_1(1) = 0$ holds. By taking into account that the two branches G_0 and G_1 coincide just at q_c, we obtain $D_{q_c} = 1$ and $q_c = z/(z-1)$. From relation (33) the well-known result [30, 21, 35, 37] $D_q = q/[z(q-1)]$ follows. Note that the slope c drops out here since $\ln c'$ is proportional to $\ln c$.

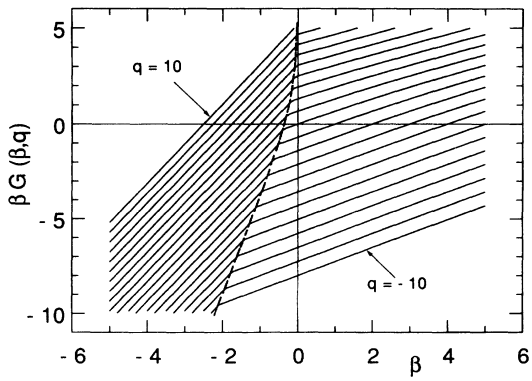

FIG. 8. The Gibbs potential for the natural measure of the map $f(x) = 1 - |2x-1|^4$. Note that the critical line (dashed) does not intersect the vertical axis; hence there is no transition in the entropies. There is a break in the D_q and λ_q spectrum at $q_c = 4/3$ and $q_c'' = 0.374$, respectively.

In contrast to the dimensions, the critical point of the Lyapunov spectrum seems to depend on details of the map. With the exception of exotic cases, however, there is *no* phase transition in the entropies, reflecting the fact that this particular spectrum is invariant under a broader class of transformations than the others.

B. Chaotic repellers

Chaotic repellers are often hyperbolic since the maxima of maps generating transient chaos lie typically outside their supports [Fig. 1(a)]. Maps consisting of two different arches separated by a cut show up in the dissipative limit of Lorenz-type systems that do *not* exhibit the usual inversion symmetry of the Lorenz model [44]. By changing the parameters in this family, one might find configurations in which the local extremum of f falls exactly on the end point of the support, as illustrated by an example in Fig. 9. Since this extremum is then mapped onto the origin that belongs obviously to the repeller, the natural measure [45,46] will be singular there, just like in cases of nonhyperbolic attractors. This mechanism then leads to a phase transition in the spectra of repellers, which has not been studied earlier. Here we first extend the formalism of the previous sections in order to include such cases, and then investigate the corresponding Gibbs potential and other spectra.

The measure map of nonhyperbolic repellers can obviously be represented by a closed function of the type shown in Fig. 1(b). Unfortunately, no simple method is known for constructing such a map. We can, however, use the fact that f itself is the measure map in regions where the density is smooth, just like for attractors, but f is now open.

Let us, therefore, consider the eigenvalue formalism for a general case where the measure map g is open. The interval lengths generated by g according to Eq. (15) are then not normalized to unity. In order to define measures we thus have to generalize the second relation of (15) as

$$P_i^{(n)} = \frac{g_i^{-n}(I)}{\sum_j g_j^{-n}(I)}. \tag{46}$$

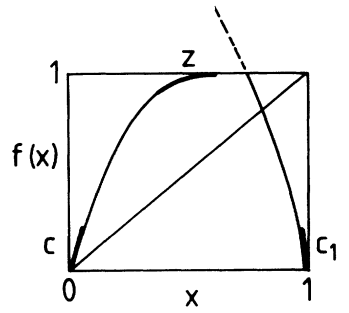

FIG. 9. Map generating a nonhyperbolic repeller as its invariant set. Notation as in Fig. 5.

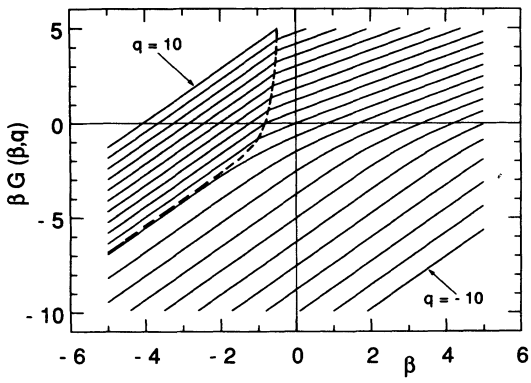

FIG. 10. The Gibbs potential for the natural measure on the repeller of the nonhyperbolic map $f(x) = 4x(1-x)$ for $x \leq 1/2$, and $f(x) = 4.5x(1-x)$ otherwise. There is a phase transition in D_q and λ_q at $q_c = 1.951$ and $q_c'' = 1$, respectively, but the entropy spectrum is smooth. The approximation (56) yields in this case $q_c = 1.956$.

The denominator decays exponentially with n, according to the free energy $F_g(\beta)$ of the measure map taken at $\beta = 1$. Thus, we can write

$$P_i^{(n)} \sim e^{\nu n} g_i^{-n}(I), \tag{47}$$

where $\nu \equiv F_g(1)$ is a positive number. The analysis of Eq. (5), as done in Sec. III A and in the Appendix, leads then, instead of (6), to

$$\lambda(\beta, q) = \exp\{[-\beta G(\beta, q) - \nu q]n\}. \tag{48}$$

This means that a trivial factor is to be taken into account when comparing the Gibbs potential and the largest eigenvalue $\lambda(\beta, q)$ of the bivariate Frobenius-Perron equation in such cases.

The invariant density $\varrho(x)$ of a repeller is the eigenfunction of the original Frobenius-Perron equation (2) taken at $\beta = 1$ with eigenvalue $\lambda(1) = \exp(-\kappa)$ [12], where $\kappa \equiv F(1)$ is the so-called escape rate characterizing the strength of repulsion of the invariant set under f. The singularity analysis of Sec. IV A then shows that $\varrho(x)$ follows a power-law behavior with an exponent $(-1 + 1/z)$ at $x = 0, 1$, but is smooth otherwise. Thus, the measures of the extremal boxes are proportional to the power $1/z$ of their size. In other boxes the measure is simply proportional to the length. As the sizes of the extremal boxes go like c^{-n} (c being the slope of f at the origin), the normalization condition can be written as

$$1 = \sum_1^{2^n} P_i^{(n)} \sim D^{(n)} \left(c^{-n/z} + (\text{const}) \sum{}' l_i^{(n)} \right). \tag{49}$$

The second term in the large parentheses [containing again a restricted summation like in (44)] is proportional to $\exp(-\kappa n)$ and always dominates the first one. This follows from the upper bound (40), which for $q = 0$, $\beta = 1$ yields $\kappa \leq \ln(c)/z$. Consequently, the normalization factor is $D^{(n)} \sim \exp(\kappa n)$. Comparing this with (47) we conclude that in case of nonhyperbolic repellers the general relation (48) holds, with the constant ν taken as the escape rate κ of the repeller.

We are now in a position to determine the Gibbs potential. The property that the measure of the first box scales as $c^{-n/z}$ means that the measure map has to have a slope $c' = c^{1/z}$ at the origin. In the condensed phase we thus obtain from (29) that

$$\lambda_0(\beta, q) = c^{-(\beta + q/z)n}, \tag{50}$$

and by means of (48) one finds

$$\beta G_0(\beta, q) = \left(\beta + \frac{q}{z}\right) \ln c - \kappa q \tag{51}$$

for the Gibbs potential.

In the hyperbolic phase, we again use the fact that the measure of intermediate boxes is proportional to their length, which leads to (44). In this phase $\lambda(\beta, q) = \lambda_1(\beta, q)$, and the application of (48) yields

$$\beta G_1(\beta, q) = sF_1(s)|_{s=\beta+q} - \kappa q. \tag{52}$$

A singularity analysis applied to the Frobenius-Perron equation of a map f like the one in Fig. 9 shows that there cannot be any phase transition in the free energy. Therefore, F and F_1 coincide and one can also use the complete $F(\beta)$ in (52) for this type of map. The Gibbs potential of a nonhyperbolic repeller obtained by using (51) and (52) is displayed in Fig. 10. It is worth mentioning that by taking the limit $\beta \to 0$, $q \to 1$ in (52), the metric entropy appears expressible via the Lyapunov exponent $\bar{\lambda}$ and the escape rate κ as $K_1 = \bar{\lambda} - \kappa$. In contrast to (14), this relation only holds for the natural measure of repellers [45].

The critical value q_c of the dimension spectrum belongs to a configuration where the branches of G_0 and G_1 intersect each other just on the β axis (Fig. 6). Thus, one obtains the condition

$$\left(\beta_c(q_c) + \frac{q_c}{z}\right) \ln c = sF_1(s)\,|_{s=\beta_c(q_c)+q_c}\,. \tag{53}$$

Due to (51), this can be converted into an implicit equation for q_c:

$$sF_1(s)\,|_{s=q_c(1-1/z+\kappa/\ln c)} = \kappa q_c, \tag{54}$$

which can be solved easily in a graphical way.

Reading off the generalized dimension in the condensed phase from (51), we obtain

$$D_q = \left(\frac{1}{z} - \frac{\kappa}{\ln c}\right) \frac{q}{q-1}. \tag{55}$$

Since the support of the measure is now an arbitrary fractal, this result is much less universal than that for attractors, and it also contains the escape rate and the slope. This dependence, of course, vanishes in the limit $\kappa \to 0$.

In the special case when the escape rate κ is small, an explicit expression can be obtained for q_c. We can then expand $\beta F(\beta)$ around $\beta = 1$ and use the fact that its derivative taken there is just the average Lyapunov exponent $\bar{\lambda}$ [see Eqs. (13) and (52)]. Keeping first-order terms in κ only, one finds

$$q_c \approx \frac{z}{z-1}\left[1 - \frac{\kappa}{z-1}\left(\frac{z}{\ln c} - \frac{1}{\bar{\lambda}}\right)\right]. \tag{56}$$

Besides the escape rate and the slope, the Lyapunov exponent $\bar{\lambda}$, too, appears here, showing again that the phase transition in the dimension spectrum of chaotic repellers is much less universal than that of attractors.

Although there is a nondifferentiability in the Lyapunov spectrum, the entropies cannot exhibit a phase transition. To see this, use upper bound (40) taken at $q = 0$ and relation (52) to write $\beta G_1(\beta, q) = (\beta/z + q/z)\ln c - \kappa q - \Delta(\beta, q)$, where Δ is positive for any finite value of its variables. From the intersection of this branch with that of G_0, one finds

$$\beta_c(q) = -\frac{z}{z-1}\frac{\Delta(\beta_c(q), q)}{\ln c}. \tag{57}$$

Since Δ is finite, this implies that the critical line cannot intersect the vertical axis at any finite q.

VI. DISCUSSION

We have investigated multifractals, the support and weight of which are generated by two different single-humped functions (Fig.1), the length scale and measure maps, respectively. The Gibbs potential $G(\beta, q)$ of such objects was shown to be closely related to the largest eigenvalue of the bivariate Frobenius-Perron equation (5), which is accessible by iterations starting from any smooth initial function. This property provides us with a numerical method to determine the Gibbs potential that is much more effective than an evaluation of the partition function after a direct measurement of length scales and weights. A singularity analysis of the iteration procedure has been applied to clarify the origin of nonanalyticity in the largest eigenvalue.

Having the possibility to choose the length scale and measure maps at will, we can draw some general conclusions concerning singular behaviors in the thermodynamic description of multifractals. Our investigations indicate that phase transitions are *generically of first order* in the Gibbs potential. There exists then a *condensed phase* where the function $\beta G(\beta, q)$ is *linear* in both variables and exhibits universal properties. Depending on the extension of the condensed phase, transitions might show up in the spectra of dimensions, entropies, and Lyapunov exponents, too. The q *dependence* of these spectra inside the condensed phase is then *unique*: dimensions and entropies must be proportional to $q/(q-1)$, while Lyapunov exponents exhibit the behavior (36).

Exceptional cases when either length scales or measures decay faster or slower than exponentially are characterized by exotic transitions. There is then a region where the function $\beta G(\beta, q)$ is completely independent of one of its variables or becomes minus infinity. This has the consequence that the dimensions and/or entropies must be identically zero or infinity in entire ranges of q. One finds that these spectra can only vanish for $q > 1$ and can only become infinite for $q < 0$. Recent investigations [43] support the view that the growth probability of DLA clusters exhibits an exotic transition characterized by the rule $D_q = K_q = \infty$ for negative q values.

For chaotic dynamical systems the natural measure is of special importance. We constructed the Gibbs potential of the natural measure for nonhyperbolic chaotic attractors of one-dimensional maps with complete topology and showed how the well-known phase transition in the dimension spectrum [30, 21, 35, 37] arises from this more general description. The novel phenomenon of phase transitions in the natural measure of nonhyperbolic chaotic repellers has been used as another example. Since the fractal dimension of the support can be any number between 0 and 1, the critical point of the dimension spectrum is less universal than for attractors. It has been shown that the entropy spectrum must be smooth, in general. If, however, the map is intermittent or extremely unstable in the origin, phase transitions in the entropies are expected to appear, just like for chaotic attractors.

Finally, it is worth briefly discussing the relation of Eq. (5) to a similar one introduced in the literature. In generalizing the fluctuation-spectrum theory of univariate time series to multivariate ones, Fujisaka and Inoue [25] have recently studied a multivariate extension of the master equation for discrete Markov processes and applied to hyperbolic cases. The bivariate version of their master equation taken with two single-humped functions f and g reads

$$\tilde{\lambda}(\beta, q) Q_{n+1}(x, y) = \sum_{\epsilon,\epsilon'(=0,1)} \frac{Q_n(f_\epsilon^{-1}(x), g_{\epsilon'}^{-1}(y))}{|f'(f_\epsilon^{-1}(x))|^\beta |g'(g_{\epsilon'}^{-1}(y))|^q}, \tag{58}$$

where $\tilde{\lambda}(\beta, q)$ is an eigenvalue. The difference between this form and Eq. (5) is that the preimages are taken here with respect to a two-dimensional noninvertible map $[x' = f(x), y' = g(y)]$ and not by prescribing the same symbolic path for x and y. Consequently, the right-hand side consists of four terms, not of two as Eq. (5). We believe that the restriction $\epsilon = \epsilon'$ leading to the bivariate Frobenius-Perron equation is *essential* when studying the thermodynamics of multifractal measures, since this is what expresses the organization of length scales and weights according to the *same* symbolic code. It is this property that also ensures that the linear operator defined by the bivariate Frobenius-Perron equation (5) is nothing but a (continuous) *transfer matrix* belonging to the elastic spin chain (with infinite range interactions) defined by the thermodynamic analogy mentioned in Sec. II.

ACKNOWLEDGMENTS

Illuminating discussions with Ch. Beck, A. Csordás, M. Eisele, P. Szépfalusy, and G. Vattay are acknowledged. One of us (T.T.) would like to thank Professor G. Eilenberger and Professor H. Kastrup for their kind hospitality at the KFA Jülich and at the RWTH Aachen, respectively. This work was partially supported by the Hungarian Academy of Sciences under Grant No. OTKA 819.

APPENDIX: DERIVATION OF THE BIVARIATE FROBENIUS-PERRON EQUATION IN NONHYPERBOLIC CASES

We first prove Eqs. (5) and (6) for the following settings. Take arbitrary seed points x^* and y^* inside the support $[0,1]$ of functions f and g, respectively. The preimages of the seed points can be arranged on a binary tree as shown in Fig. 11. The coordinates at level n are given by

$$x^{(n)}(\epsilon_n,\epsilon_{n-1},\ldots,\epsilon_1) = F_{\epsilon_1}\circ F_{\epsilon_2}\circ\cdots\circ F_{\epsilon_n}(x^*),$$
$$y^{(n)}(\epsilon_n,\epsilon_{n-1},\ldots,\epsilon_1) = G_{\epsilon_1}\circ G_{\epsilon_2}\circ\cdots\circ G_{\epsilon_n}(y^*), \tag{A1}$$

where the string $\{\epsilon_i\}, \epsilon_i = 0$ or 1, defines the symbolic path along which a given preimage is taken. Note, however, that neighboring points of these symbolic trees are not at all close to each other in coordinate space.

It is an interesting feature of single-humped maps that by using the particular tree defined by Fig. 11 the coordinates become ordered according to their magnitudes if they are put on the same tree but with *symbol sequences reversed*. This property is independent of hyperbolicity, and Fig.12 shows an elementary example.

Consider now such position-ordered representations of the symbolic trees. Let us define two coverages of the support $I = [0,1]$, with respect to the presentation functions F and G, via the intervals $h^{(n)}$ and $k^{(n)}$, respectively, specified by points, the codes of which differ in their *last digits* only (see Fig. 13). The lengths of these intervals are thus

$$h^{(n)}(\epsilon_1,\ldots,\epsilon_{n-1}) \equiv |\, F_{\epsilon_1}\circ F_{\epsilon_2}\circ\cdots\circ F_{\epsilon_{n-1}}\circ F_1(x^*) - F_{\epsilon_1}\circ F_{\epsilon_2}\circ\cdots\circ F_{\epsilon_{n-1}}\circ F_0(x^*)\,|,$$
$$k^{(n)}(\epsilon_1,\ldots,\epsilon_{n-1}) \equiv |\, G_{\epsilon_1}\circ G_{\epsilon_2}\circ\cdots\circ G_{\epsilon_{n-1}}\circ G_1(y^*) - G_{\epsilon_1}\circ G_{\epsilon_2}\circ\cdots\circ G_{\epsilon_{n-1}}\circ G_0(y^*)\,|. \tag{A2}$$

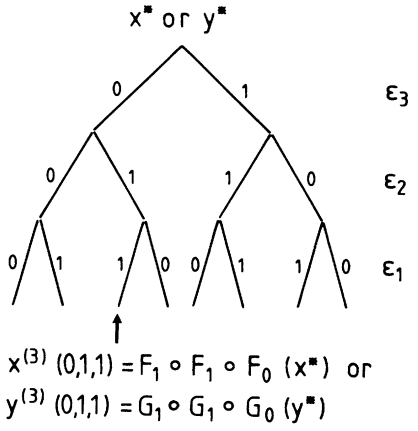

FIG. 11. Binary tree and labeling used in the Appendix. The points $x^{(n)}$ or $y^{(n)}$ are obtained from the seed points x^* or y^*, respectively, as a composition of the presentation functions F_ϵ or G_ϵ, in the order shown. By using this convention, the last digit ϵ_n is the least relevant in determining the position of a point [see also Fig. 12(b)].

Consider the partition function (3) built up on these quantities as length scales and measures, i.e., take

$$l_i^{(n)} = h^{(n)}(\epsilon_1,\ldots,\epsilon_{n-1}),\quad P_i^{(n)} = D^{(n)}k^{(n)}(\epsilon_1,\ldots,\epsilon_{n-1}), \tag{A3}$$

where $D^{(n)}$ is a normalization factor. Asymptotically, for large n it becomes constant if g is closed; otherwise, $D^{(n)} \sim \exp(\nu n)$ with $\nu = F_g(1)$, as given by (47). Apart from this distinction, both the length scale and measure maps can be either open or closed. Here we restrict our attention to the most nonhyperbolic case when f and g are both closed, as shown in Fig. 1(b), and possess smooth maxima. If one of the maps is hyperbolic, an analogous derivation holds.

An analysis of partition sum (3) can then be performed very much in the same way as that of partition function (1) [18]. The essential observation in deriving Eq. (5) is that the length scales and measures (A3), defined pictorially in Fig. 13, can be expressed as products of the presentation functions' derivatives. The length scales $l_i^{(n)}$ and measures $P_i^{(n)}$ decrease as $n \to \infty$, which formally follows from (A2) by using the fact that the n-fold iterated maps f^n, g^n are expanding at any point away from the preimages of 1. (This also shows that the seed points x^*, y^* can freely be chosen from the middle part of the support $[0,1]$.) One can thus replace the differences in (A2) by the derivatives of $F_{\epsilon_1}, G_{\epsilon_1}$. As the total func-

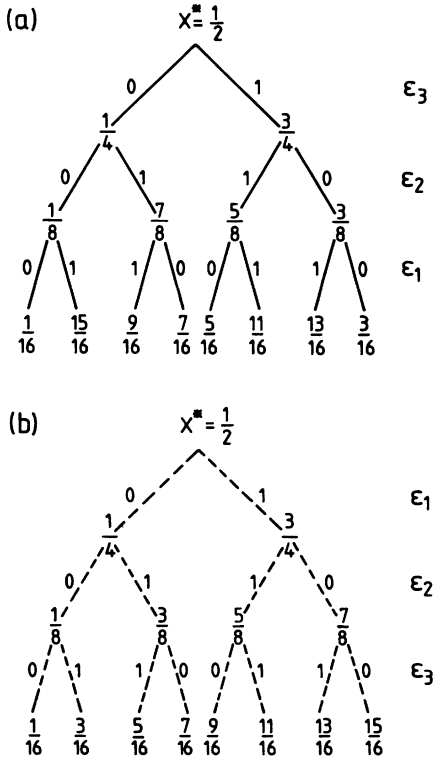

FIG. 12. Example of a binary tree (a) and its position-ordered version (b), up to level $n = 3$. The particular map used is $f(x) = 1 - |\,2x - 1\,|$.

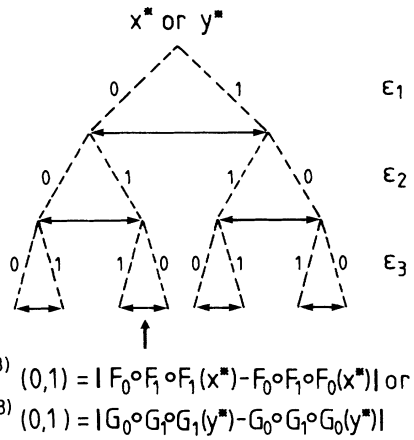

FIG. 13. Position-ordered tree and the definition of intervals $h^{(n)}$ and $k^{(n)}$ (arrows), the sizes of which can be taken as length scales and measures, respectively, in partition sum (3).

tions acting on the seed points are compositions, a subsequent application of the chain rule leads to the appearance of the presentation function's derivatives with subscripts $\epsilon_2, \epsilon_3, \ldots$, too. One cannot go, however, back to the seed points, since the differences $F_0(x^*) - F_1(x^*)$ and $G_0(y^*) - G_1(y^*)$ are not at all small. We, therefore, have to stop after applying the chain rule $m < n$ times, reaching level $n - m$ where the coordinate differences are still small. The number $n - m$ can be large but *fixed* so that when taking the limit $n \to \infty$ level m also goes to infinity. One then can write

$$
\begin{aligned}
h^{(n)}(\epsilon_1,\ldots,\epsilon_{n-1}) &= |\, F'_{\epsilon_1}(F_{\epsilon_2}\circ F_{\epsilon_3}\circ\cdots\circ F_{\epsilon_m}(\hat{x})) \\
&\quad \times F'_{\epsilon_2}(F_{\epsilon_3}\circ\cdots\circ F_{\epsilon_m}(\hat{x}))\cdots F'_{\epsilon_m}(\hat{x})\,| \\
&\quad \times h^{(n-m)}(\epsilon_{m+1},\ldots,\epsilon_{n-1}), \\
k^{(n)}(\epsilon_1,\ldots,\epsilon_{n-1}) &= |\, G'_{\epsilon_1}(G_{\epsilon_2}\circ G_{\epsilon_3}\circ\cdots\circ G_{\epsilon_m}(\hat{y})) \\
&\quad \times G'_{\epsilon_2}(G_{\epsilon_3}\circ\cdots\circ G_{\epsilon_m}(\hat{y}))\cdots G'_{\epsilon_m}(\hat{y})| \\
&\quad \times k^{(n-m)}(\epsilon_{m+1},\ldots,\epsilon_{n-1}),
\end{aligned}
\tag{A4}
$$

where $h^{(n-m)}$ and $k^{(n-m)}$ are defined as in (A2) but now contain $m+1$ as the first ϵ subscript. The coordinates with hats are shorthand notations for

$$
\begin{aligned}
\hat{x} &\equiv F_{\epsilon_{m+1}}\circ F_{\epsilon_{m+2}}\circ\cdots\circ F_{\epsilon_n}(x^*), \\
\hat{y} &\equiv G_{\epsilon_{m+1}}\circ G_{\epsilon_{m+2}}\circ\cdots\circ G_{\epsilon_n}(y^*).
\end{aligned}
\tag{A5}
$$

Since the difference $n - m$ is large, it is practically irrelevant if the last code ϵ_n is 1 or 0, and both $h^{(n-m)}$ and $k^{(n-m)}$ are small numbers.

Next, consider the sum

$$
S(n,\beta,q) = \sum_{i=1}^{2^{n-1}} \lambda^{-n+1}(\beta,q) l_i^{(n)\beta} P_i^{(n)q}, \tag{A6}
$$

which—in view of (3) and (4)—is of the order of unity, provided

$$
\lambda(\beta,q) = \exp[-\beta G(\beta,q)] \tag{A7}
$$

is chosen. After substituting (A3) and (A4) we can rearrange (A6) as

$$
\begin{aligned}
S(n,\beta,q) = \lambda^{m-n+1}(\beta,q) \sum_{\epsilon_{n-1},\ldots,\epsilon_{m+1}} & h^{(n-m)\beta}(\epsilon_{m+1},\ldots,\epsilon_{n-1}) k^{(n-m)q}(\epsilon_{m+1},\ldots,\epsilon_{n-1}) \\
&\times \sum_{\epsilon_m} \lambda^{-1}(\beta,q)\,|\,F'_{\epsilon_m}(\hat{x})\,|^{\beta}\,|\,G'_{\epsilon_m}(\hat{y})\,|^{q} \\
&\times \sum_{\epsilon_{m-1}}\cdots\sum_{\epsilon_1} \lambda^{-1}(\beta,q)\,|\,F'_{\epsilon_1}(F_{\epsilon_2}\circ\cdots\circ F_{\epsilon_m}(\hat{x}))\,|^{\beta} \\
&\times |\,G'_{\epsilon_1}(G_{\epsilon_2}\circ\cdots\circ G_{\epsilon_m}(\hat{y}))\,|^{q}\,.
\end{aligned}
\tag{A8}
$$

For $n, m \to \infty$ the right-hand side is an infinite product of sums taken over the symbols $\epsilon_1, \ldots, \epsilon_m$. To proceed, consider a partial product containing summations over $\epsilon_1, \ldots, \epsilon_{r-1} (m > r \to \infty)$, and adopt the following notation:

$$
\begin{aligned}
&Q_r(F_{\epsilon_{r+1}}\circ F_{\epsilon_{r+2}}\circ\cdots\circ F_{\epsilon_n}(x^*), G_{\epsilon_{r+1}}\circ G_{\epsilon_{r+2}}\circ\cdots\circ G_{\epsilon_n}(y^*)) \\
&\qquad \equiv \sum_{\epsilon_r} \lambda^{-1}(\beta,q)\,|\,F'_{\epsilon_r}(F_{\epsilon_{r+1}}\circ\cdots\circ F_{\epsilon_n}(x^*))\,|^{\beta}\,|\,G'_{\epsilon_r}(G_{\epsilon_{r+1}}\circ\cdots\circ G_{\epsilon_n}(y^*))\,|^{q} \sum_{\epsilon_{r-1}}\cdots .
\end{aligned}
\tag{A9}
$$

After introducing

$$
\begin{aligned}
x &\equiv F_{\epsilon_{r+2}}\circ F_{\epsilon_{r+3}}\circ\cdots\circ F_{\epsilon_n}(x^*), \\
y &\equiv G_{\epsilon_{r+2}}\circ G_{\epsilon_{r+3}}\circ\cdots\circ G_{\epsilon_n}(y^*),
\end{aligned}
\tag{A10}
$$

the terms standing to the right of $\sum_{\epsilon_r}$ in (A8) yield precisely $Q_{r+1}(x,y)$. Also, written explicitly, these terms can be expressed as

$$
\begin{aligned}
Q_{r+1}(x,y) = \lambda^{-1}(\beta,q) \sum_{\epsilon} & \,|\,F'_{\epsilon}(x,y)\,|^{\beta}\,|\,G'_{\epsilon}(x,y)\,|^{q} \\
&\times Q_r(F_{\epsilon}(x), G_{\epsilon}(y)).
\end{aligned}
\tag{A11}
$$

Using the fact that the inverses of the length scale and measure maps are the presentation functions [see (19)], one immediately sees that this is just the bivariate Frobenius-Perron equation (5). Since with choice (A7) sum $S(n,\beta,q)$ stays of the order of unity as n grows, Q_r

must be a well-defined function on $[0,1]$ for any value of r.

Considering Q_1 as defined by (A9) for $r=1$ and comparing this with (A11), Q_1 appears as the first iterate of a constant function $Q_0 \equiv 1$. This implies that the iteration of the bivariate Frobenius-Perron equation starting from any *smooth* initial distribution converges towards a finite limiting function $Q(x,y)$ if the largest eigenvalue is related to the Gibbs potential as $\lambda(\beta,q) = \exp[-\beta G(\beta,q)]$, where $G(\beta,q)$ can also be obtained from partition sum (3) evaluted with length scales and measure as defined by (A3).

Finally, we extend the result to the partition used in the text generated by the preimages of the unit interval taken with respect to maps f and g [see (15)]. Consider the sets of length scales and measures defined as

$$\tilde{l}_i^{(n)} = f_i^{-n+1}(I), \quad \tilde{P}_i^{(n)} = g_i^{-n+1}(I), \tag{A12}$$

$i = 1,\ldots,2^{n-1}$. One easily convinces oneself that the sizes of the intervals $f_i^{-n+1}(I)$ and $g_i^{-n+1}(I)$ are longer than $l_i^{(n)}$ and $P_i^{(n)}$ of (A3), respectively, at any fixed n,i. Furthermore, each long interval of the set (A12) *contains* one element from partition (A3). Therefore, the *scaling* of $l_i^{(n)}$ and $\tilde{l}_i^{(n)}$, as well as of $P_i^{(n)}$ and $\tilde{P}_i^{(n)}$, must be identical when changing n. Thus, we conclude that the $G(\beta,q)$ obtained via Eqs. (5) and (6) also coincides with the Gibbs potential of partition sum (3) when the length scales and measures are taken as the preimages of $[0,1]$ according to Eq. (15).

---

* Permanent address: Institute for Theoretical Physics, Eötvös University, Budapest.

[1] Y.G.Sinai, Usp.Mat.Nauk. **27**, 21 (1972) [Russ. Math. Surveys **166**, 21 (1972)]; R.Bowen, *Equilibrium States and the Ergodic Theory of Anosov Diffeomorphisms*, Lecture Notes in Mathematics Vol. 470 (Springer, Berlin, 1975), p. 1; D. Ruelle, *Thermodynamic Formalism* (Addison-Wesley, Reading, MA, 1978); D. H. Mayer, *The Ruelle-Araki Transfer Operator in Classical Statistical Mechanics*, Lecture Notes in Physics Vol. 123 (Springer, Berlin, 1980).

[2] M. J. Feigenbaum, M. H. Jensen, and I. Procaccia, Phys. Rev. Lett. **56**, 1503 (1986); D. Ruelle, *ibid.* **56**, 405 (1986); J. Stat. Phys. **56**, 405 (1986).

[3] M. Sano, S. Sato, and M. Sawada, Prog. Theor. Phys. **76**, 945 (1986).

[4] M. Kohmoto, Phys. Rev. A **37**, 1345 (1987).

[5] T. Bohr and D. Rand, Physica D **25**, 387 (1987).

[6] M. H. Jensen, L. P. Kadanoff, and I. Procaccia, Phys. Rev. A **36**, 1409 (1987); M. J. Feigenbaum, J. Stat. Phys. **46**, 919 (1987); **46**, 925 (1987); P. Collet, J. Lebowitz, and A. Porzio, *ibid.* **47**, 609 (1987); P. Alström, in *Time-Dependent Effects in Disordered Materials*, edited by R. Pynn and T. Riste (Plenum, New York, 1987); D. H. Mayer, Phys. Lett. **121A**, 390 (1987); D. H. Mayer and G. Roepstorff, J. Stat. Phys. **47**, 149 (1987); **50**, 331 (1988); T. Bohr and T. Tél, in *Directions in Chaos*, edited by U. Bai-lin Hao (World Scientific, Singapore, 1988), Vol. II, pp. 195–237; A. Arneodo and M. Holschneider, J. Stat. Phys. **50**, 995 (1988); D. Bessis *et al.*, J. Stat. Phys. **51**, 109 (1988).

[7] T. Tél, Z. Naturforsch. **43A**, 1154 (1988).

[8] A. B. Chhabra, R. V. Jensen, and K. R. Sreenivasan, Phys. Rev. A **40**, 4593 (1989).

[9] R. Badii, Riv. Nouvo Cimento **12**, 1 (1989); V. Baladi, J-P. Eckmann, and D. Ruelle, Nonlinearity **2**, 119 (1989); R. Artuso, E. Aurell, and P. Cvitanović, *ibid.* **3**, 325 (1990); **3**, 361 (1990); F. Christiansen, G. Paladin, and H. H. Rugh, Phys. Rev. Lett. **65**, 2087 (1990); C. Beck, Physica D **50**, 1 (1991); J. Bene (unpublished).

[10] P. Szépfalusy and T. Tél, Phys. Rev. A **34**, 2520 (1986); T. Tél, Phys. Lett. **A119**, 65 (1986).

[11] T. Tél, Phys. Rev. A **36**, 2507 (1987).

[12] T. Tél, Phys. Rev. A **36**, 1502 (1987).

[13] P. Szépfalusy and U. Behn, Z. Phys. B **65**, 337 (1987).

[14] H. Fujisaka and M. Inoue, Prog. Theor. Phys. **78**, 268 (1987).

[15] A. Csordás and P. Szépfalusy, Phys. Rev. A **38**, 2582 (1988).

[16] M. J. Feigenbaum, J. Stat. Phys. **52**, 527 (1988).

[17] I. Procaccia and R. Zeitak, Phys. Rev. Lett. **50**, 2511 (1988); S. Vaienti, J. Phys. A **21**, 2023 (1988); **21**, 2313 (1988); J. Bene, Phys. Rev. A **39**, 2090 (1989); Z. Kovács, J. Phys. A **22**, 5161 (1989); H. Mori *et al.*, Prog. Theor. Phys. **81**, 60 (1989); T. Kobayashi *et al.*, Prog. Theor. Phys. **82**, 1 (1989); P. Gaspard and S. A. Rice, J. Chem. Phys. **90**, 2225 (1989); **90**, 2242 (1989); M. R. Michalski, Ph.D. thesis, Virginia Polytechnic Institute, 1990 (unpublished); H. Fujisaka and H. Shibata, Prog. Theor. Phys. **85**, 187 (1991); Lj. Kocarev and Z. Tasev (unpublished); G. Vattay (unpublished).

[18] M. J. Feigenbaum, I. Procaccia, and T. Tél, Phys. Rev. A **39**, 5359 (1989).

[19] Z. Kovács and T. Tél, Phys. Rev. A **40**, 4641 (1989).

[20] P. Szépfalusy, T. Tél, and G. Vattay, Phys. Rev. A **43**, 681 (1991).

[21] T. C. Halsey *et al.*, Phys. Rev. A **33**, 1141 (1986).

[22] T. Vicsek, *Fractal Growth Phenomena* (World Scientific, Singapore, 1989); R. E. Amritkar and N. Gupte, in *Directions in Chaos*, edited by Hao Bai-lin (World Scientific, Singapore, 1989), Vol. 3, pp. 227–362; P. Meakin, Prog. Solid State Chem. **20**, 135 (1990).

[23] H. G. E. Hentschel and I. Procaccia, Physica **8D**, 435 (1983).

[24] N. Gupte and R. E. Amritkar, Phys. Rev. A **39**, 5466 (1989); **41**, 4285 (1990).

[25] H. Fujisaka and M. Inoue, Phys. Rev. A **41**, 5302 (1990).

[26] X.-J. Wang, Phys. Rev. A **40**, 6647 (1989); A. Porzio, J. Stat. Phys. **58**, 923 (1990); P. Collet, R. Dobbertin, and P. Moussa (unpublished).

[27] C. Maneveau, K. R. Sreenivasan, P. Kailasnath, and M. S. Fan, Phys. Rev. A **41**, 894 (1990); C. Maneveau and A. B. Chhabra, Physica **164A**, 564 (1990); S. J. Lee and T. C. Halsey, *ibid.* **164A**, 575 (1990).

[28] R. Cawley and R. D. Mauldin, Adv. Appl. Math. (to be published).

[29] R. Stoop, J. Parisi, and H. Brauchli, Z. Naturforsch **46a**, 642 (1991); R. Stoop and J. Parisi, Phys. Lett. A (to be published); R. Stoop, J. Peinke, and J. Parisi, Physica **50D**, 405 (1991); R. Stoop (unpublished).

[30] E. Ott, W. Withers, and J. A. Yorke, J. Stat. Phys. **36**, 697 (1984).
[31] P. Cvitanović, in *Group Theoretical Methods in Physics*, edited by R. Gilmore (World Scientific, Singapore, 1987), pp. 37–54; P. Szépfalusy and T. Tél, Phys. Rev. A **35**, 477 (1987); D. Katzen and I. Procaccia, Phys. Rev. Lett. **58**, 169 (1987); R. Badii and A. Politi, Phys. Rev. A **35**, 1288 (1987); Phys. Scr. **35**, 243 (1987); P. Szépfalusy, T. Tél, A. Csordás, and Z. Kovács, Phys. Rev. A **36**, 3525 (1987); M. H. Jensen and T. Bohr, *ibid.* **36**, 4904 (1987).
[32] T. Horita *et al.*, Prog. Theor. Phys. **80**, 793 (1988); H. Hata *et al.*, *ibid.* **80**, 809 (1988); T. Yoshida *et al.*, *ibid.* **82**, 879 (1989).
[33] P. Grassberger, R. Badii, and A. Politi, J. Stat. Phys. **51**, 135 (1988); E. Ott, C. Grebogi, and J. A. Yorke, Phys. Lett. A **135**, 343 (1989).
[34] A. Csordás and P. Szépfalusy, Phys. Rev. A **39**, 4767 (1989).
[35] Hao Bai-lin, *Elementary Symbolic Dynamics* (World Scientific, Singapore, 1989, Sec. 6.2.2); F. H. Ling, Phys. Lett. **A138**, 25 (1989).
[36] X.-J. Wang, Phys. Rev. A **39**, 3214 (1989); A. Csordás and P. Szépfalusy, Phys. Rev. A **40**, 2221 (1989); Z. Kaufmann and P. Szépfalusy, Phys. Rev. A **40**, 2615 (1989); J. Bene, P. Szépfalusy, and A. Fülöp, Phys. Rev. A **40**, 6719 (1989); S. Sato and K. Honda, Phys. Rev. A **42**, 3233 (1990); W. Just, Phys. Lett. **150A**, 362 (1990); P. Kluiving, H.W. Capel, and R.A. Pasmanter, Physica **164A**, 594 (1990); K. Honda, S. Sato, and H. Kodama, Phys. Rev. A **43**, 2669 (1990); A. O. Lopes (unpublished).
[37] C. Beck, Physica D **41**, 67 (1990).
[38] R. Stoop and J. Parisi, Phys. Rev. A **43**, 1802 (1991).
[39] P. Grassberger and I. Procaccia, Phys. Rev. A **28**, 2591 (1983); J.P. Eckmann and D. Ruelle, Rev. Mod. Phys. **67**, 617 (1985); J.P. Eckmann and I. Procaccia, Phys. Rev. A **34**, 659 (1986).
[40] H. Fujisaka, Prog. Theor. Phys. **70**, 1264 (1983); **71**, 513 (1984).
[41] P. Grassberger, in *Chaos*, edited by A. Holden (Manchester University Press, Manchester, 1986), pp. 291–311.
[42] G. Györgyi and P. Szépfalusy, Z. Phys. B. **55**, 179 (1984).
[43] T. Bohr, P. Cvitanović, and M. H. Jensen, Europhys. Lett. **6**, 445 (1988); J. Lee and H. E. Stanley, Phys. Rev. Lett. **61**, 2945 (1988); S. Schwarzer *et al.*, *ibid.* **65**, 603 (1990); B. B. Mandelbrot, Physica **168A**, 95 (1990); B. B. Mandelbrot, C. J. Evertsz, and Y. Hayakawa, Phys. Rev. A **42**, 4528 (1990); J. Lee *et al.*, *ibid.* **42**, 4832 (1990).
[44] P. Szépfalusy and T. Tél, Physica **16D**, 252 (1985); Z. Kaufmann *et al.*, Acta Phys. Hung. **62**, 321 (1987).
[45] H. Kantz and P. Grassberger, Physica **17D**, 75 (1985).
[46] T. Tél, in *Direction in Chaos*, edited by Bai-lin Hao (World Scientific, Singapore, 1990), Vol. 3, pp. 149–211.